COMPRESSIVE SENSING RADAR: SIMULATION AND EXPERIMENTS FOR TARGET DETECTION

L. Anitori, W. van Rossum, M. Otten

A. Maleki

R. Baraniuk

TNO,
The Hague, The Netherlands

Columbia University, New York City, USA Rice University, Houston, USA

ABSTRACT

In this paper the performance of a combined Constant False Alarm Rate (CFAR) Compressive Sensing (CS) radar detector is investigated. Using the properties of the Complex Approximate Message Passing (CAMP) algorithm, it is demonstrated that the behavior of the CFAR processor can be separated from that of the non-linear ℓ_1 -norm recovery, thus allowing the use of standard radar equations to evaluate detection performance. The CS CFAR processor has been evaluated under different interference scenarios using both the Cell Averaging (CA) and Order Statistic (OS) CFAR detectors. The performance of the CS CFAR processor is also compared to that of an ℓ_1 -norm detector using both simulations and experimental data.

Index Terms— Compressive Sensing, Complex Approximate Message Passing, Radar, Detection, CFAR.

1. INTRODUCTION

Compressive Sensing (CS) is a novel data acquisition scheme, which enables reconstruction of sparse signals from undersampled measurements. Sparsity of the signals can reasonably be assumed in many radar applications where the number of resolution cells is much higher than the number of targets present in the scene. Examples of CS applied to radar can be found in [1–5].

To perform adaptive target detection, classical radar architectures use well-established processing methods, such as Matched Filtering (MF) and Constant False Alarm Rate (CFAR) processors. In CS instead, the reconstruction of the target scene involves the use of highly nonlinear algorithms based on ℓ_1 -norm minimization. Such algorithms have a number of free parameters (or thresholds) that must be tuned properly to achieve good performance and whose values depend on both the underlying noise power and the number of targets. Therefore, in a practical scenario, with neither the disturbance variance nor the number of targets known a priori, it is not evident how to tune these parameters to achieve the desired detection/false alarm performance.

To deal with the uncertainties about the background noise and interference, CFAR processors are used in most operational radars for adaptive target detection [6, 7]. In such schemes, some assumptions are made about the underlying noise (and clutter) distribution in order to set the appropriate threshold to achieve the desired detection and False Alarm Probabilities (FAP). Instead, the design of CFAR-like schemes in combination with CS recovery is not straightforward, due to the non-linearity of CS recovery algorithms and the unknown relations between the noise statistics and the parameters involved in the ℓ_1 -norm reconstruction. However, in a series of recent publications [5, 8], the authors demonstrate that by exploiting the properties of the Complex Approximate Message Passing (CAMP) algorithm, classical CFAR processing can be successfully combined with ℓ_1 -minimization to obtain a fully adaptive detection scheme.

In this paper, the performance of the joint CS CFAR detector, in combination with both the Cell Averaging (CA) and the Order Statistic (OS) CFAR processors, are investigated under different interference scenarios using simulated as well as experimental CS radar measurements.

2. COMPLEX APPROXIMATE MESSAGE PASSING (CAMP)

CS deals with the problem of recovering a k-sparse signal $\mathbf{x_0} \in \mathbb{C}^N$ from an undersampled set of linear measurements $\mathbf{y} \in \mathbb{C}^n$, with n < N, of the form

$$y = Ax_0 + n. (1)$$

Here, $\mathbf{A} \in \mathbb{C}^{n \times N}$ is the sensing matrix, and \mathbf{n} is complex white Gaussian noise with variance σ_{in}^2 .

Since in the CS framework the number of measurements n is smaller than the number of signal samples N, the problem of recovering $\mathbf{x_0}$ is ill-posed. However, under certain conditions on \mathbf{A} , n, and k the following convex optimization problem, known as the LASSO [9] or Basis Pursuit Denoising (BPDN) [10], recovers a close approximation of $\mathbf{x_0}$ [11]:

$$\widehat{\mathbf{x}} = \min_{\mathbf{x}} \frac{1}{2} \|\mathbf{y} - \mathbf{A}\mathbf{x}\|_{2}^{2} + \lambda \|\mathbf{x}\|_{1}.$$
 (2)

Here, λ is a regularization parameter that controls the trade off between the sparsity of the solution and the ℓ_2 -norm of

the residual. A major practical problem when dealing with CS reconstruction algorithms is finding the "optimal" value of λ . In particular, for radar applications the relations between the parameter λ and the detection and false alarm probabilities are unknown.

The Complex Approximate Message Passing (CAMP) is an iterative algorithm for solving (2) for signals in the complex domain [5, 12]. The CAMP algorithm has a number of properties which can be used to solve both the problem of optimal tuning and adaptive target detection. These properties are summarized in P1–P3 [12]:

- P1: Under an appropriate tuning of the regularization parameter used in CAMP and the parameter λ in (2), CAMP solves LASSO exactly. See Section 3.4 in [12].
- P2: At every iteration, $\tilde{\mathbf{x}}^t$ can be considered as $\mathbf{x_0} + \mathbf{w}^t$, where the distribution of \mathbf{w}^t converges to complex Gaussian with zero mean and variance σ_t^2 . See Section 3.4 in [12].
- P3: The performance of CAMP can be predicted theoretically by the so-called state evolution equation. See Section 3.1 in [12].

An important relation derived from the analytical framework used in CAMP is that the variance of the total noise σ_t^2 present in the signal $\tilde{\mathbf{x}}$ at each iteration t is expressed as a linear combination of the input noise variance and the MSE of the solution: $\text{MSE}_t = \frac{\|\hat{\mathbf{x}}^t - \mathbf{x}_0\|^2}{N}$. In CAMP an estimate $\hat{\sigma}_t^2$ of the noise variance is computed at each iteration by means of median filtering.

With the use of the signal-plus-noise model described in P2, the tuning of the regularization parameter in CAMP, which we refer to as τ , can be easily solved. The optimal threshold τ_o in CAMP is the one that achieves the minimum MSE or, equivalently, the minimum σ_∞^2 . The *Adaptive CAMP* algorithm described in [8] can be used to obtain a good estimate $\hat{\tau}_o$ of the optimal threshold multiplier τ_o when signal and noise statistics are unknown. The optimum estimated threshold $\hat{\tau}_o$ minimizes the estimated CAMP output noise variance thus maximizing the recovery SNR of CAMP (and therefore the P_d of any detector that may follow the recovery stage).

3. CS TARGET DETECTION USING CAMP

In radar, the detection problem is to determine the presence or absence of a target in a given range/Doppler bin in the presence of noise, clutter and interference. In practice, the background is unknown a priori, and therefore an adaptive detection scheme must be applied. Also, it is desirable that the detector has the CFAR property, which can be achieved by using CFAR detection on the signal $\tilde{\mathbf{x}}$. Two different CS CAMP based architectures are considered here and their block diagrams are shown in Figure 1.

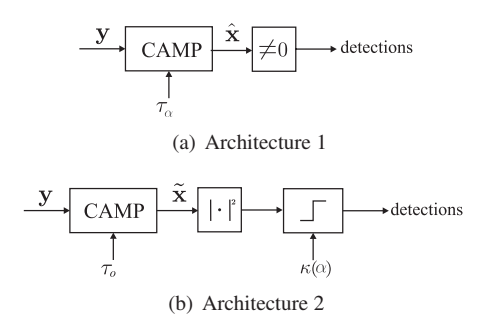


Fig. 1. Detection schemes based on CAMP. Note that in Architecture 2 the output of CAMP is the noisy version of the estimated signal $\tilde{\mathbf{x}}$.

In the first system, the CS reconstruction itself is considered to act as a detector, and the non-zero coefficients in the estimated signal $\widehat{\mathbf{x}}(\tau_{\alpha})$ represents detections. Therefore, the threshold τ_{α} in CAMP is set to achieve the desired FAP α . In [5] it is shown that for $\mathbf{x_0}=0$, setting the threshold $\tau_{\alpha}=\sqrt{-\ln\alpha}$ yields a FAP equal to α . This detection strategy is referred to as Architecture 1; see Figure 1(a).

Theoretical and empirical results in [8] show that better performance can be achieved in terms of detection probability (P_d) when the CS recovery is followed by a separate detector. This means that, similar to conventional radar processing, the recovery stage - a Matched Filter (MF) in classical architectures- is used to maximize the recovery SNR (i.e., maximize detection for a given FAP), and later the detector is used to control the FAP. In this case the CAMP threshold is selected to achieve the minimum MSE at the output of CAMP by choosing $\tau=\tau_o$, with τ_o estimated using Adaptive CAMP. This scheme is referred to as Architecture 2; see Figure 1(b). In this architecture, the input to the separate detector is the non-sparse, noisy signal $\tilde{\mathbf{x}}$.

4. CFAR DETECTORS

If the noise statistics were homogeneous, stationary and known, the detector threshold in both architectures could be set once and would remain fixed. This represents the ideal case of a fixed threshold (FT) detector. These conditions are never satisfied in practice and CFAR processors are employed to adaptively estimate the detector threshold $\kappa(\alpha)$ when the background statistics are not known in advance. In CFAR schemes the cell under test (CUT) is tested for the presence of a target against a threshold derived from the estimated clutter-plus-noise power. The M cells surrounding the CUT (CFAR window) are used to derive an estimate of the background power and they are assumed to be target free. CFAR schemes try to maintain a constant false alarm rate via adaptation of the threshold to a changing environment. It is known that for the case of homogeneous Gaussian background, the optimum CFAR processor is the well-known Cell Average

CFAR (CA-CFAR) detector [6]. However, in situations in which the clutter changes rapidly or in the presence of interfering targets in the CFAR window, or when the clutter and noise distribution are not Gaussian, the CA-CFAR detector performance degrades severely. For this reason many alternative CFAR schemes have been developed in the past, such as the Order Statistic (OS) CFAR detector [7]. In OS-CFAR processing, the power received from the cells in the CFAR window is rearranged in increasing order and the *k*th ordered cell (order statistic) is used as an estimate of the environment. OS-CFAR processing has the advantage of being robust against interfering targets in the CFAR window and clutter power transitions, while preserving reasonably good performance in homogenous background.

5. SIMULATION

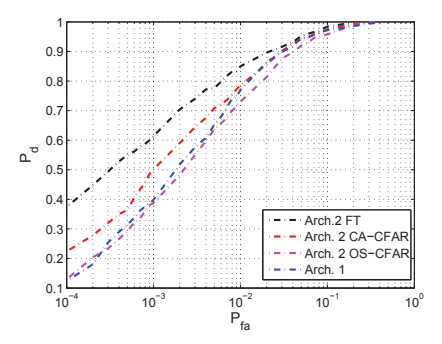
A stepped frequency (SF) waveform is considered for simulations and the TX signal consisted of a number of discrete frequencies f_m . In the CS case, the number of TX frequencies is reduced from N to n (n < N). The subset of transmitted frequencies is chosen uniformly at random within the total transmitted bandwidth, with the constraints that the first and last frequencies in the bandwidth are used (to span the same total bandwidth to preserve range resolution), and that at least two of the transmitted frequencies are separated by the nominal frequency separation Δf , to guarantee that the unambiguous range ΔR is preserved. After reception and demodulation each range bin maps to n phases proportional to the n transmitted frequencies, and the n samples y_m , $m = 1, \dots, n$, of the compressed measurement vector \mathbf{y} are given by

$$y_m = \frac{1}{\sqrt{n}} \sum_{i=1}^{N} e^{-j4\pi f_m r_i/c} x_{0,i},$$
 (3)

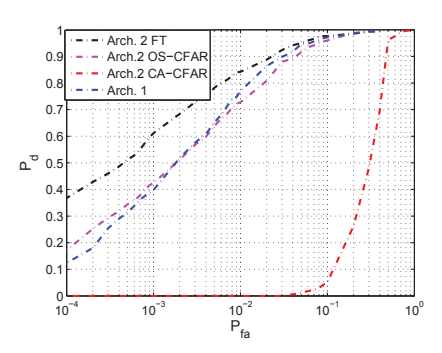
where $r_i = r_0 + i \Delta R/N$, and i = 1, ..., N is the range bin index.

5.1. Simulation results

The simulation results are shown in Figure 2, where the detection performance are shown for both Architecture 1 and for Architecture 2 using a Fixed Threshold (FT) detector and a CFAR processor, either a CA or OS one. The detection probability (P_d) is estimated using 500 Monte Carlo simulations for a target with a recovery SNR of about 9 dB. The design FAP on the x-axis (P_{fa}) is used to set the threshold multiplier for each architecture and detector type. In the simulations, the case N=1000, $\delta=0.5$ and $\rho=0.1$ is considered, where $\delta=n/N$ indicates the number of CS measurements wrt the number of Nyquist samples and $\rho=k/n$ represents the relative signal sparsity, being k the number of targets. The targets are distributed in range such that, depending on the CFAR window length M, the target of interest (for which the P_d is



(a) CFAR window length M=20



(b) CFAR window length M=40

Fig. 2. ROC curves for a target with a recovery SNR of about 9 dB using Architecture 1 (blue), and Architecture 2 in combination with FT detector (black), CA-CFAR (red), and OS-CFAR (magenta) processors. For the OS-CFAR processor, $k_{OS}=0.6$. In these simulations, N=1000, $\delta=0.5$ and $\rho=0.1$.

shown) has either no interfering targets (M=20) or 2 interferers (M=40) in its CFAR window.

From Figure 2 it can be seen that, in agreement with traditional CFAR processing, the CA CFAR processor outperforms the OS one for the case of homogeneous background in the CFAR window (2(a)). Instead, when interferers are present in the CFAR window, the CA processor encounters a significant loss in P_d compared to the OS processor, whose performance is almost unaffected by in the presence of interfering targets in the CFAR window.

Also note that for all detector cases (adaptive and non-adaptive), the CAMP reconstruction threshold τ_o of Architecture 2 is always adaptive, whereas in Architecture 1 the threshold τ_α is non-adaptive and fixed. Furthermore, the performance of the two architectures are upper bounded by the performance of Architecture 2 that uses an ideal (non-adaptive) fixed threshold (FT) detector that does not suffer from estimation loss instead of a CFAR one. Furthermore, because the threshold τ_α in Architecture 1 is estimated using a median estimator, the performance of this architecture is similar to those of the Architecture 2 combined with the OS

6. EXPERIMENTAL DATA

In the this section, the performance of the proposed detection schemes under different interference scenarios is evaluated using a set of experimental CS radar measurements. In the experiments, a one dimensional radar is considered operating in the range domain.

The measurements were carried out at Fraunhofer FHR, in Germany, using the LabRadOr experimental radar system described in [5]. In the Nyquist case (that represents unambiguous mapping of ranges to phases over the whole bandwidth) N=200 frequencies are transmitted using a SF waveform over a bandwidth of 800 MHz which yields a maximum range resolution of $\delta_R=18.75$ cm. Each frequency is transmitted over $0.512~\mu s$, corresponding to a bandwidth of $B_f=1.95$ MHz. The sequential frequencies are separated by $\Delta f=4$ MHz, resulting in an unambiguous range of $\Delta R=37.5$ m. Five stationary corner reflectors with different Radar Cross Sections (RCS) are used as targets. For each transmitted waveform 300 measurements (with the same setup) were performed.

6.1. Results

In this section, ROC curves are used to analyze the performance of the two architectures for both interfering and non-interfering target scenarios, which were obtained by changing the CFAR window size. For Architecture 2, we combine the CAMP recovery with both the CA and OS CFAR processors.

Figure 3 exhibits the signals reconstructed by using the two CAMP based architectures introduced in Section 3 in addition to the MF, which represent the reference case. For the CS measurements $\delta=0.5$ is used and N=200 frequencies measurements for the MF. There are five corner reflectors (T1–T5) at ranges from 20m to 36m. For Architecture 1, τ_{α} was set using $\alpha=10^{-4}$. Notice that the signal from Architecture 2 is a noisy version of the estimated sparse signal before soft thresholding is applied, whereas the signal estimated from Architecture 1 is the sparse signal, where each non-zero coefficient represents a detection.

In the interest of space, only the ROC curves for target T3 are reported. For the other targets, the behavior of the detectors is the same, although the actual values of P_d are different due to the different SNRs of both the desired target and the interferers. For estimating P_d , the detection at the location of the highest target peak was used. For Architecture 2 both the CA and OS CFAR processors were used, preceded by a Square Law (SL) detector. For the CFAR processors, we use four guard cells and CFAR windows of length 20 and 40 respectively. For the OS CFAR, the selected order statistic is chosen as $k_{OS}=0.6$.

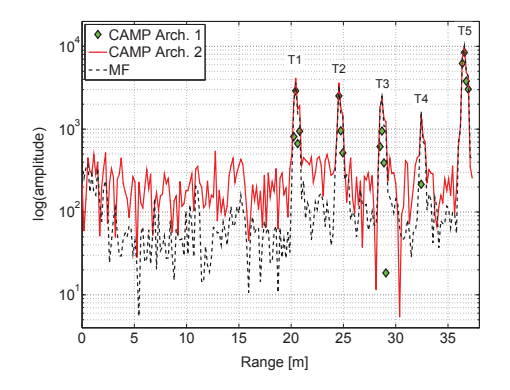
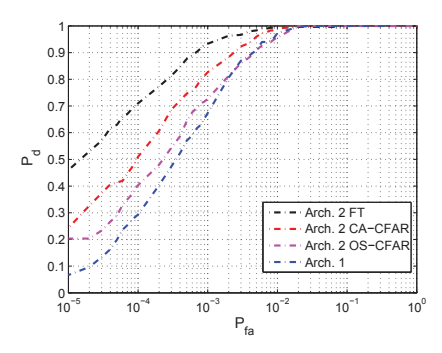


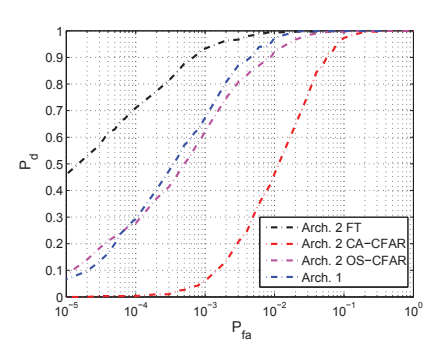
Fig. 3. Reconstructed range profile using CAMP Architectures 1 and 2, and the MF. For the MF, N=200 (i.e., no subsampling); for all other schemes n=100 and $\delta=0.5$. The y-axis is in log scale and arbitrary units [au].

Figure 4(a) shows the ROC curve for T3 with a CFAR window of length M=20. For this choice of M, none of the other targets fall in the CFAR window of T3, and therefore the CA-CFAR processor performs better than the OS one. Furthermore, it can be seen that Architecture 2 combined with the CA-CFAR processor also outperforms Architecture 1, where the noise variance is estimated inside the CAMP algorithm using the median estimator. Therefore, Architecture 1 is similar to an OS CFAR processor that uses the entire range response as the CFAR window and $k_{OS} = 0.5$. Clearly, in this case the CA CFAR performs better than both the OS CFAR and Architecture 1, since it excludes the other targets from the (local) estimation of the noise level, resulting in an unbiased estimate. For this window size, CA CFAR is the best choice since there are no noise/clutter power transitions, and the targets are never in the reference window of one another.

Figure 4(b) shows the results for the same data set but for a CFAR window of size 40, which result in 2 interfering targets in the CFAR window of the target of interest. It can be observed that, in accordance with conventional CFAR processing, Architecture 2 with OS CFAR outperforms Architecture 2 with CA CFAR but performs very similarly to Architecture 1. In fact, the performance of the CA-CFAR processor degrades as the number of interfering targets in the reference window increases. Note that the ROC curve of Architecture 1 (and also Architecture 2 with FT detector) is unchanged for different CFAR window sizes. In fact, for Architecture 1 no CFAR processor is used and the CAMP reconstruction is independent of the locations of the targets, as it uses the whole range response. It is clear that, in cases where there might be multiple interfering targets either an OS-CFAR processor should be used after Architecture 2 or otherwise the theoretically suboptimum Architecture 1 can represent a simple, effective alternative to CFAR processing. However, the disadvantage of Architecture 1 is that it lacks the local adap-



(a) CFAR window length M=20



(b) CFAR window length M=40

Fig. 4. ROC curves for T3 using Architecture 1 (blue), and Architecture 2 in combination with FT detector (black), CA-CFAR (red), and OS-CFAR (magenta) processors. For the OS-CFAR processor, $k_{OS}=0.6$. $\delta=0.5$.

tivity provided by CFAR processing. Clearly, there is a trade off between the number of range bins used for the noise power estimation and the bias in the estimate that occurs if interfering targets are included in the reference window. Of course, this trade off is identical to the trade off for classical radar systems using Nyquist sampling.

7. CONCLUSIONS

In this paper the results of different CS based radar detection architectures were compared. It is shown that using a separate detector following the CS reconstruction improves detection performance. Moreover, if the detector is a CFAR one, its behavior is unaltered and, in the presence of interfering targets in the CFAR window, as expected, OS is better than CA-CFAR processing. Furthermore, although the performance of Architectures 1 and Architecture 2 plus OS-CFAR are similar, Architecture 2 is preferable as it leaves the user the freedom to chose the most appropriate processing parameters and it allows to perform a local adaptation of the threshold, which is critical for radar applications. With the combined CS CFAR architecture, the CFAR loss can be controlled by changing both the type of CFAR processor and the window length.

Acknowledgment

The authors would like to thank Prof. J. Ender and T. Mathy from Fraunhofer FHR, Wachtberg, Germany, for making available the radar system and for technical support during the experiments.

8. REFERENCES

- [1] R. G. Baraniuk and T. P. H. Steeghs, "Compressive radar imaging," in *Proc. IEEE Radar Conf.*, 2007.
- [2] M. A. Herman and T. Strohmer, "High-resolution radar via compressed sensing," *IEEE Trans. Signal Process.*, vol. 57, no. 6, pp. 2275–2284, 2009.
- [3] J. H. G. Ender, "On compressive sensing applied to radar," *Elsevier J. Signal Process.*, vol. 90, no. 5, pp. 1402–1414, May 2010.
- [4] L. C. Potter, E. Ertin, J. T. Parker, and M. Cetin, "Sparsity and compressed sensing in radar imaging," *Proc. IEEE*, vol. 98, no. 6, pp. 1006–1020, Jun. 2010.
- [5] L. Anitori, A. Maleki, M. Otten, R. G. Baraniuk, and P. Hoogeboom, "Design and analysis of compressive sensing radar detectors," *IEEE Trans. Signal Process.*, vol. 61, no. 4, pp. 813–827, Feb. 2013.
- [6] P. P. Gandhi and S.A. Kassam, "Analysis of CFAR processors in homogeneous background," *IEEE Trans. Aerosp. Electron. Syst.*, vol. 24, no. 4, pp. 427–445, Jul. 1988
- [7] H. Rohling, "Radar CFAR thresholding in clutter and multiple target situations," *IEEE Trans. Aerosp. Electron. Syst.*, vol. 19, no. 4, pp. 608–621, Jul. 1983.
- [8] L. Anitori, A. Maleki, W. van Rossum, R. Baraniuk, and M. Otten, "Compressive CFAR radar detection," in *Proc. IEEE Radar Conf.*, 2012.
- [9] Robert Tibshirani, "Regression shrinkage and selection via the LASSO," *J. Roy. Stat. Soc., Series B*, vol. 58, no. 1, pp. pp. 267–288, 1996.
- [10] S.S. Chen, D.L. Donoho, and M.A. Saunders, "Atomic decomposition by basis pursuit," *SIAM J. on Sci. Computing*, vol. 20, pp. 33–61, 1998.
- [11] E. Candès and T. Tao, "Near optimal signal recovery from random projections: Universal encoding strategies?," *IEEE Trans. Inf. Theory*, vol. 52, no. 12, pp. 5406–5425, Dec. 2006.
- [12] A. Maleki, L. Anitori, Y. Zai, and R. G. Baraniuk, "Asymptotic analysis of complex LASSO via complex approximate message passing (CAMP)," *IEEE Trans. Inf. Theory*, vol. 59, no. 7, pp. 4290–4308, Jul. 2013.